

1 Long-term monitoring of transformation from pastoral to agricultural land use 2 using time-series Landsat data in the Feija Basin (Southeast Morocco)

3
4
5
6 4 Atman Ait Lamqadem¹, Hafid Saber¹, Biswajeet Pradhan^{**2}

7 5 ¹Laboratory of Geodynamic and Geomatics, Department of Geology, Faculty of Sciences, Chouaib Doukkali,
8 6 Morocco

9 7 ²Centre for Advanced Modelling and Geospatial Information Systems (CAMGIS), Faculty of Engineering and
10 8 Information Technology, University of Technology Sydney, 2007 NSW, Australia
11 9 Email. Biswajeet.Pradhan@uts.edu.au or Biswajeet24@gmail.com (Corresponding author)

14 15 11 Abstract

16 12 The expansion of agricultural land at the cost of pastoral land is the common cause of land degradation
17 13 in the arid areas of developing countries, especially in Morocco. This study aims to assess and monitor
18 14 the transformation of pastoral land to agricultural land in the arid environment of the Feija Basin
19 15 (Southeast of Morocco) and to find the key drivers and the issues resulting from this transformation.
20 16 Spectral mixture analysis was applied to multi-temporal (1975–2017) and multi-sensor (i.e. Multi-
21 17 spectral Scanner, Thematic Mapper, and Operational Land Imager) Landsat satellite images, from
22 18 which land use classifications were derived. The remote sensing data in combination with ground
23 19 reference data (household level), groundwater and climate statistics were used to validate and explain
24 20 the derived land use change maps. The results of the spatiotemporal changes in agricultural lands show
25 21 two patterns of changes, a middle expansion from 1975-2007, and a rapid expansion from 2008 to 2017.
26 22 In addition, the overall accuracy demonstrated a high accuracy of 94.4%. In 1975 and 1984, the
27 23 agricultural lands in Feija covered 0.17 km² and 1.32 km², respectively, compared with 20.10 km² in
28 24 2017. Since the adoption of the Green Morocco Plan in 2008, the number of watermelon farms and wells
29 25 has increased rapidly in the study area, which induced a piezometric level drawdown. The results show
30 26 that spectral mixture analysis yields high accuracies for agricultural lands extraction in arid dry lands
31 27 and accounts for mixed pixels issues. Results of this study can be used by local administrators to prepare
32 28 an effective environmental management plan of these fragile drylands. The proposed method can be
33 29 replicated in other regions to analyse land transformation in similar arid conditions.

34 30 **Keywords:** Land use monitoring; Landsat images; Linear-Mixture Analysis; GIS; Remote sensing;
35 31 Morocco

32 33 1. Introduction

34 34 The population of the world has been growing rapidly in recent years, especially in Asian and
35 35 African countries (FAO, 2017). In most developing countries, the changes in land use are
36 36 mainly due to the intense population pressure and changes in the socioeconomic situation of
37 37 the population. Human activities can change the structure and the biological capacity of
38 38 ecosystems over a period of time (Long et al., 2010). Accordingly, the effect of anthropogenic
39 39 impact on the biological ecosystems can be found through the identification and monitoring of
40 40 the land cover alterations (Teixido et al., 2010). These man-made changes are one of the major
41 41 causes of environmental degradation in any landscape (Ait Lamqadem et al., 2018).

42 The expansion of cultivated areas can mitigate the increasing demand for food, especially in
43 developing countries. Therefore, agricultural lands are most vulnerable to changes under
44 climate variabilities, political strategies and human pressures (Hamad et al., 2018). However,
45 some adverse effects of this rapid expansion emerge, especially in arid areas (Foley et al., 2011).
46 One of the major effects on the environment is the groundwater drawdown (Tilman and Clark,
47 2015). However, in the arid regions of Morocco and due to heavy government subsidies (under
48 the Green Morocco Plan since 2008), agricultural lands have been expanded on former pastoral
49 lands in recent years (Faysse, 2015).

50 Pastoral land use has been considered one of the traditional economic activities in arid regions.
51 The Feija Basin, Central-South-Eastern Morocco, presents an example of pastoral land use.
52 Nevertheless, this arid pastoral communal land underwent several environmental
53 transformations, such as the expansion of agricultural lands instead of the traditional pastoral
54 activities.

55 In the last four decades, remote sensing data inherit the potential to map and monitor these
56 environmental changes on various spatial and temporal scales (Ait Lamqadem et al., 2017;
57 Allbed et al., 2014; Tang et al., 2017; Xie et al., 2017). Changes in the land use/land cover can
58 be monitored and assessed using the historical data from the Landsat program using a
59 multispectral scanner (MSS) which started in 1972 until the current operational land imager
60 (OLI) in 2017 (Medjani et al., 2017; Zhu, 2017). Derived thematic maps can provide spatial
61 information on historical data, thereby serving as a valuable source, for example in the land use
62 and degradation monitoring of ecosystems (Xofis and Poirazidis, 2018; Zhang et al., 2018).
63 Remote sensing data can be used to monitor the land use changes, specifically transformations
64 from pastoral to agricultural uses (Kartya et al., 2005; McPeak and Little, 2018). Comparing
65 satellite imagery from different Landsat sensors can be a challenge due to varying sensor types.
66 A Spectral Mixture Analysis (SMA) technique was applied to overcome this problem (Schmidt
67 et al., 2003). Several studies have proved that SMA can monitor land-cover/land-use changes
68 in arid and semi-arid environments (Adams et al., 1995; Dawelbait et al., 2017; Salih et al.,
69 2017). SMA, as a subpixel classification, produces fractions or abundances of the different
70 features of surfaces (Scarth et al., 2010). Endmembers are required as inputs to the unmixed
71 different components of the surface.

72 However, only a few studies on the arid areas of South-Eastern Morocco to detect the effects
73 and the drivers of the specific types of land use changes are available. Consequently, an urgent
74 need to monitor and assess the land use dynamics emerges. Therefore, this study aims to assess

75 and monitor the land use changes and analyse the possible change-driving forces and the impact
76 of the transition from pastoral land use to an agricultural land use. Accordingly, multispectral
77 and multitemporal Landsat satellite data (i.e. MSS, thematic mapper (TM) and OLI) from 1975
78 to 2017 were used. SMA was used to extract the extent of agricultural land use in the Feija
79 Basin at the time of the study.

80 2. Study Area

81 The sub-basin of Feija is part of the Middle Draa Valley (MDV). The MDV is located in the
82 central-southern part of Morocco, middle of the 06° west meridian and below the 30° north
83 parallel. The basin of Draa has an area of approximately 14380 km² and a width of 1200 km,
84 crossed by Draa Wadi (typical ephemeral river), the longest wadi in Morocco. The basin is fed
85 by the Mansour Eddahbi Dam upstream MDV, constructed in 1972. The Draa river forms a
86 chain of six successive oases, varying from 100 m to 10 km in width (Mezguita, Tinzouline,
87 Ternata, Fezouata, Ktaoua and M'Hamid) (**Fig. 1**).

88 Geographically, the Feija Basin (2270 km²) is located in the southern foot slopes of the high
89 Atlas Mountains in South Morocco. It stretches approximately 80 km from west to east and 8
90 to 12 km from north to south. Feija is part of the Fezouata Basin and situated at the west of the
91 River Draa near Zagora Town (**Fig. 1**). The sector of the study is characterized by arid climate
92 with an average of 70 mm of annual precipitation equivalent to 15 days of rain. The potential
93 evapotranspiration is high, reaching 2500 mm/year (Schmidt et al., 2003). Temperatures can
94 reach more than 48 °C in the summer and varies between -1 and 7 °C in the winter (Ait
95 Lamqadem et al., 2018). The hydrological system depends on the extent of water runoff in the
96 central Anti-Atlas. In traditional oases (Mezguita to M'Hamid), the agricultural system usually
97 consists of three production levels, namely, date palm trees (*Phoenix dactylifera*), fruit trees
98 and surface-level vegetables (i.e. tomatoes, maize, alfalfa and henna) (Ait Lamqadem et al.,
99 2019). Outside of the palm oases, the surface-level system is the main agricultural system
100 (henna, wheat and watermelon). Furthermore, the extensive mobile pastoralism on collective
101 land is the traditional form of land use in the Feija area (Schmidt et al., 2003). This is the
102 rationale behind selecting this basin as a study area.

103 Over centuries and decades, pastoralism in arid areas has been considered a crucial economic
104 activity and a method of land exploitation (Zainabi, 1989). Goats, sheep and dromedaries are
105 the main livestock in the study site.

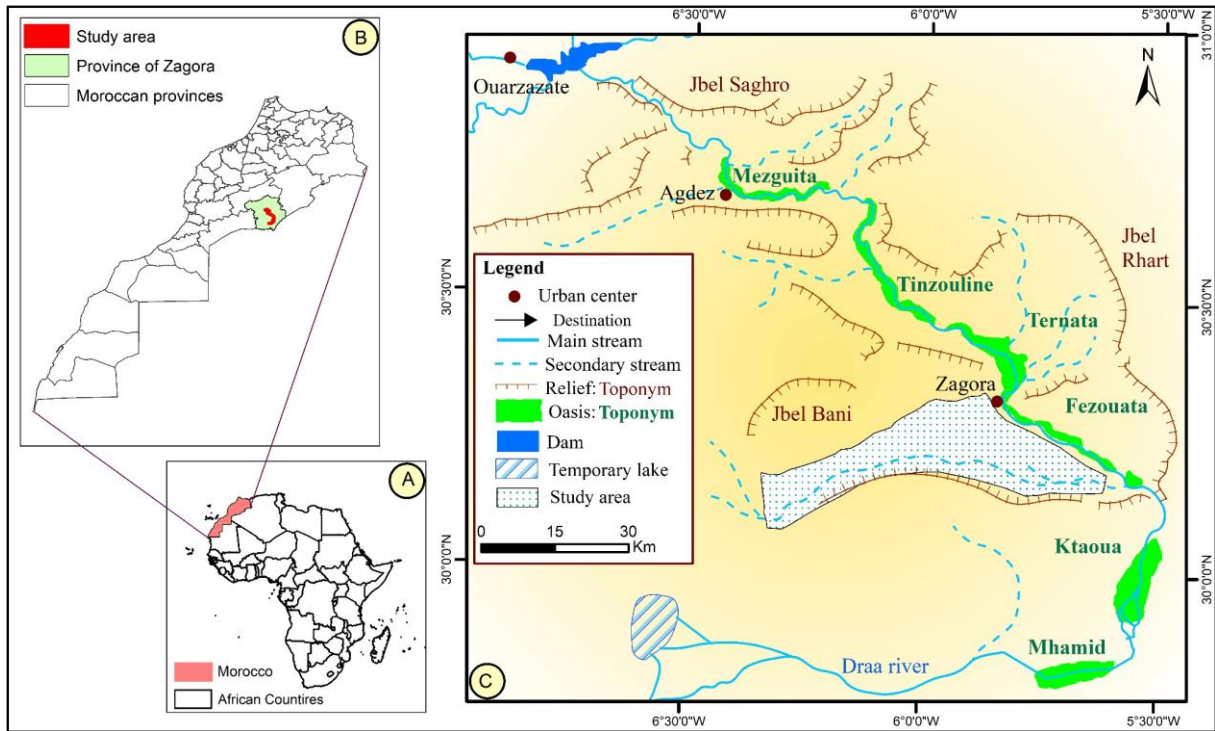


Fig. 1. Location map of study area: (A) Morocco in Africa; (B) study area in Zagora Province; and (C) study area.

Water for agricultural purposes is directly pumped from private wells. The productivity of the groundwater is between 1 and 5 l/s with some exceptional zones where it reaches 40 l/s. In addition, traditional and drip irrigation systems are adopted in the Feija Basin. The soil consists of the lacustrine sediments that show fine textures and low skeleton contents, favouring water holding properties and the possibility of mechanical treatment (Klose, 2009).

Historically, the sedentarisation in the Feija Basin (settling of a nomadic population) started in 1970 because of the advances in well technologies. Livestock and agriculture are the main socioeconomic activities in the Feija.

The figure 2 shows the main land cover/land use in the study area.

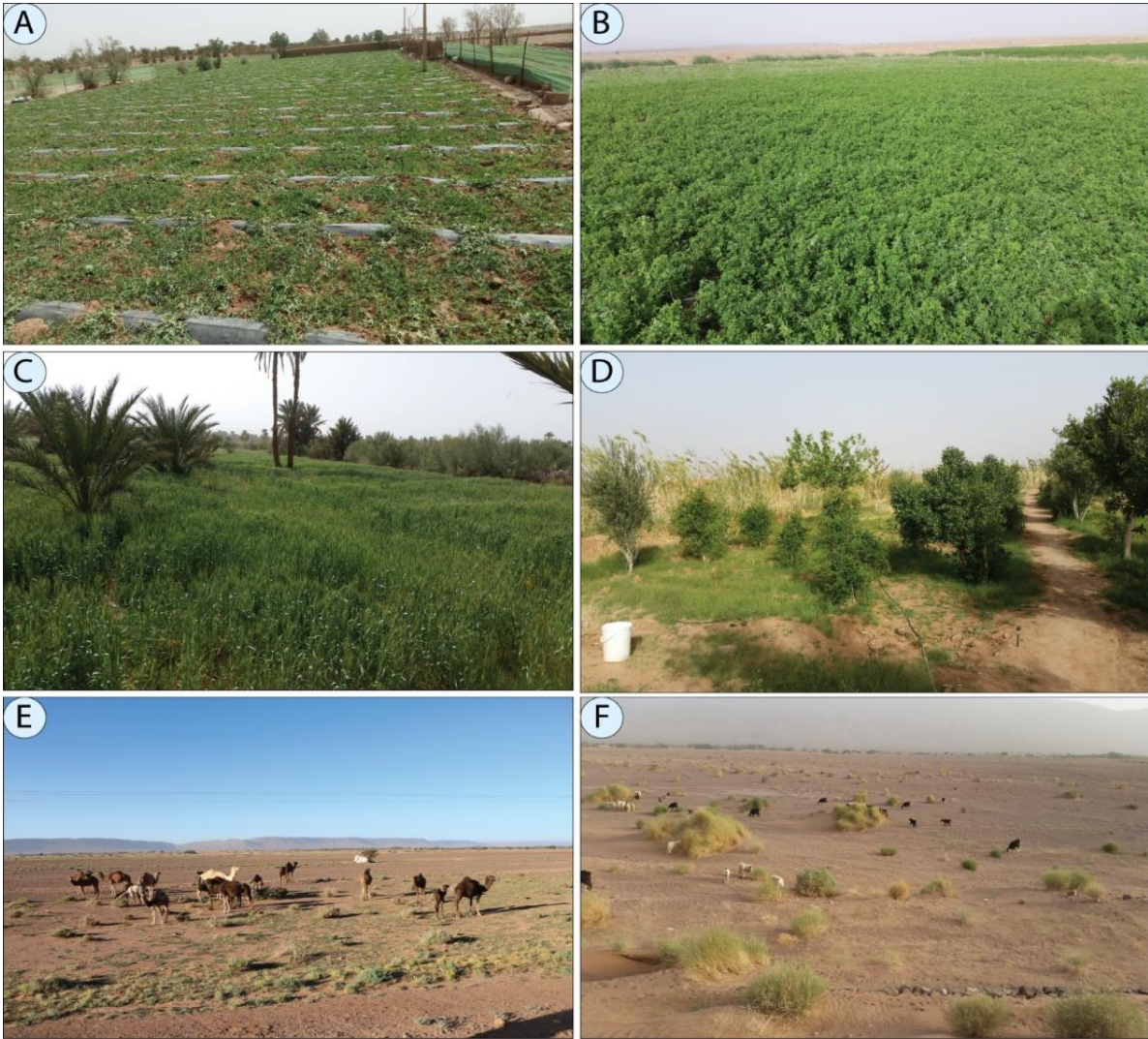


Figure 2. (A) Watermelon fields; (B): Alfalfa fields; (C) Wheat fields; (D) Fields with fruit trees; (E) and (F): Pastoral lands.

3. Data

The data used in this study include the remote sensing images, fractional vegetation field measurements and ancillary data.

3.1. Remote sensing data

Three multispectral image sets from Landsat Multispectral Scanner (MSS), Landsat 5 Thematic Mapper (TM) and Landsat 8 Operational land Imager (OLI) were collected. Georectification Level 1 Precision Terrain (L1TP) Landsat from 1975 to 2017 images with less than 10% cloud coverage were downloaded freely online from the U.S. Geological Survey platform (<https://earthexplorer.usgs.gov/>). The radiometric resolutions for the Landsat MSS and TM sensors were 8 bits, while the radiometric resolution of Landsat OLI sensor was 16 bits. Table 1 describes the main characteristics of the used images. The linear spatial resolution of MSS image is 79 by 79

132 meters. For Landsat 5 TM and Landsat 8 OLI images, the native resolution is 30 m. The selected
 133 period is from May to June (except 1975), which coincides best with a full ground cover of
 134 watermelon, cropped from January to June. This period was also chosen to avoid confusion and
 135 interference with the annual vegetation and agricultural cycles. Landsat images represent the
 136 only source of global, calibrated and moderate spatial resolution measurements of the Earth's
 137 surface with the longest lifespan among Earth Observation Systems that are preserved in a
 138 national archive and freely available to the public (<https://landsat.usgs.gov/landsat-8-18-data-users-handbook-section-1>). Furthermore, the L1TP products made available by the provider
 139 allow the user to have immediate access to ready-to-use high quality products suitable for pixel-
 140 level time series analysis without further pre-processing.

142 **Table 1.** Description of the used Landsat data.

Satellite	Sensor	Spatial resolution (m)	Acquired date	Cloud cover (%)	Path	Raw
Landsat 1	MSS	79	03-July-1975	0.00	216	39
		30	14-May-1984	0.00	200	39
Landsat 5	TM	30	03-May-2000	0.00	200	39
			30-May-2007	0.00	200	39
			10-Juin-2011	0.00	200	39
			30-May-2013	0.00	200	39
Landsat 8	OLI	30	02-June-2014	0.00	200	39
			20-May-2015	0.08	200	39
			22-May-2016	0.07	200	39
			25-May-2017	0.00	200	39

143 3.2. Field data collection

144 Fieldwork was conducted in the Feija Basin between April and May 2017. Preliminary
 145 topographic map and high-resolution images from Google Earth were used to identify the
 146 candidate areas to be surveyed, and the appropriate paths. In addition, agricultural lands, rocks,
 147 pastoral lands, sand, partial vegetation coverage and water plots were identified during
 148 fieldwork.

149 An economical, efficient and high-speed method to estimate the vegetation fraction coverage
 150 is the use of a digital camera (Han and Han, 2015). In total, 38 plots were collected in the field
 151 using the vertical photography method, with an altitude of one meter. The chosen elementary
 152 size of sample plots matched with the spatial resolution of the Landsat images perfectly (30m
 153 × 30 m). An area size of 1 m² quadrant was selected and the photos were taken vertically using
 154 a Nikon D90 digital camera. Every plot was registered using a Garmin eTrex GPS, with 2

155 meters of precision, to allow integration with the other spatial data in the GIS and image
156 processing systems. The vegetation percentage of each image was extracted after geometric
157 correction, enhancement processing, colour space transformation and classification (Li et al.,
158 2015), which used the ISODATA-unsupervised classification algorithm in ENVI Exelis Harris
159 Geospatial Solutions Software. In addition, 14 subclasses were determined to classify each
160 photograph, and then the subclasses were combined to derive the bare land, nonphotosynthetic
161 and photosynthetic vegetation. This method was previously validated and applied to extract the
162 fractional vegetation coverage (Li et al., 2015; White et al., 2000; Zhang et al., 2013). The
163 samples were randomly collected in the field. The data were collected in different land cover
164 types in the study area (agricultural land, palm grove, sparse vegetation, and bare land). A
165 portion of the collected samples was used to assess the accuracy of the fractional vegetation
166 coverage extracted by the SMA subpixel model and the land use classification (agricultural vs.
167 nonagricultural) and the remaining portion for the validation of the results.

168 Field data also consisted of semi-structured interviews with the pastoralists. The interviews
169 focused on the main motivations of the process of sedentisation from a pastoral to an
170 agricultural land use. The semi-structured interview is a method of qualitative study based on
171 the performance of the individual or collective interviews during which the facilitator dictates
172 only the different topics to be addressed without asking specific questions (Ait Lamqadem et
173 al., 2019).

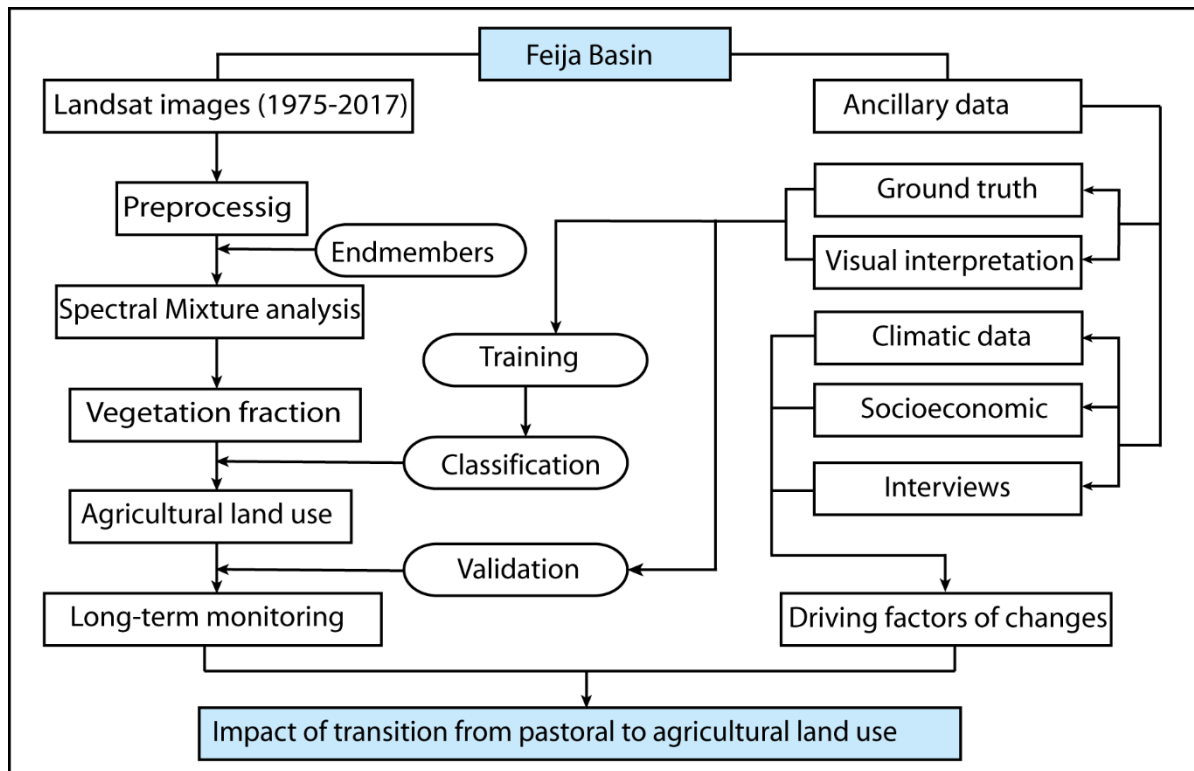
3.3. Ancillary data

174 The ancillary data were used to analyse the driving forces of the vegetation changes. The
175 climatic and socioeconomic data were provided from different administrations. The climatic
176 data were acquired from the Office Régional de Mise en Valeur Agricole de Ouarzazate
177 (ORMVAO). The household level data were provided through interviews with local residents
178 and government administrators.

179 Water samples were also collected during the field survey in the Feija Area with the aim to
180 measure the salinity of the water. The water well was collected in different bottles and then the
181 salinity was measured. Water salinity was measured through electrical conductivity. The
182 electrical conductivity (mS cm^{-1}) of the water samples was measured using a conductometer at
183 25 °C (Yıldırım and Öner, 2015).

4. Methodology

186 The adopted methodology in this study is divided into three main stages (**Fig. 3**). Firstly, the
 187 collection and pre-processing of Landsat images include co-registration check and atmospheric
 188 correction to assure the spatial and spectral consistency of multi-date images. Secondly, this
 189 stage includes the application of spectral mixture analysis and then the extraction of agricultural
 190 land use. Lastly, this stage includes the exploitation of ancillary data to evaluate the effects of
 191 the agricultural land use evolution and to discuss the driving forces of changes.



192 **Fig. 3.** Methodological flowchart.

193
 194 *4.1. Landsat images and pre-processing*

195 The downloaded images contain high-quality L1TP. The images selected in this research were
 196 radiometrically normalized to obtain the top of atmosphere reflectance by the USGS (Guo et
 197 al., 2017; Mihi et al., 2017). Subsequently, dark object subtraction (Mantinfar et al., 2012; Pons
 198 et al., 2014) was applied for atmospheric correction, thereby obtaining surface reflectance.
 199 Landsat images were converted from digital numbers to surface reflectance through rescaling
 200 in accordance with the instructions of the provider (Afrasinei et al., 2018). Given the
 201 characteristics of the study area, no topographic correction was applied because L1TP was
 202 orthorectified using ground control points and a digital elevation model to correct the relief
 203 displacement (Afrasinei et al., 2018). Therefore, the geometric correction was unnecessary for
 204 L1TP (Roy et al., 2014). Landsat MSS image was resampled to the native resolution of Landsat
 205 OLI using the nearest neighbourhood algorithm (Ait Lamqadem et al., 2018).

4.2. Spectral mixture analysis

SMA has been widely used as one of the most efficient models to assess and monitor vegetation coverage in arid and semiarid environments (Masoud, 2014; Meusbürger et al., 2010; Smith et al., 1990). In comparison with the other classification techniques, such as support vector machine or artificial neural network, which offer high accuracy, SMA is more effective for subpixel classification, especially for the differentiation of vegetation and soil (Wang et al., 2010). Further, the ranges of the spectral bands are different, as with the case of the sensors of the Landsat program (MSS, TM, and OLI). Furthermore, their ratios (NDVI and SAVI), as most vegetation indices, are also not directly comparable. The most common approach in SMA is to apply post-classification change detection (Schmidt et al., 2003).

In the satellite images of arid and semi-arid areas, the pixels usually contain mixed spectral reflectance due to the variability in the distribution of different feature components on the surface. SMA is based on the presumption that the spectral reflectance of each pixel is a function of the weighted average of the objects within it (Dawelbait et al., 2017).

SMA uses endmembers to transform the radiance or reflectance of the image into abundances or fractions (Elmore et al., 2000). The resulting image of the SMA is an image, with each band representing an endmember abundance (Adams et al., 1986; Smith et al., 1985).

To perform SMA involves the evaluation of specific features in the image to extract the endmembers (pure pixels) and the selection of physical features. Lastly, the step allows the determination of fraction for each selected endmember.

SMA was adopted due to its ability to compare the data acquired from different sensors, i.e. MSS, TM and OLI. SMA was performed with ENVI (ITT Exelis, USA) with the sum to unity constraints, which means that the sum of the endmember fraction for each pixel equals to one. The values of each fraction vary between 0 (0% of the material) and 1 (100% of the material).

4.3. Endmembers extraction

The selection of endmembers (pure pixels) is one of the most crucial stages in performing SMA (Lu, 2006). Endmember collection can be approached from the field or library, also known as the library endmember (Smith et al., 1990), or the selection of spectra directly from the image (image endmember). In this study, the image-based method was performed to extract endmembers. The image endmember is easier to perform compared with the library endmember, which needs calibration between selected endmembers and the spectra measured in the field or laboratory (Lu, 2006).

238 For the extraction of endmembers and the development of high-quality fraction images,
239 different image transformations can be used, such as principal components and minimum noise
240 fraction (MNF). Several automated methods commonly used to extract endmembers (geometric
241 perspective and pixel purity index [PPI]) employ PCA or MNF to reduce the dimensionality of
242 data and image noise (Fernández-Manso, 2015). We determined the candidate endmembers by
243 analysing the PPI. This algorithm has been widely used in hyperspectral image analysis for
244 endmember extraction. The MNF was applied to each Landsat image, and then we connect the
245 MNF transformation with the PPI using an n-dimensional visualization tool to apply n-
246 dimensional visualization analysis and extract the spectral information of all the components
247 (Han and Han, 2015). The four endmembers defined in the study are vegetation, sand, clay and
248 rock.

249 *4.4. Agricultural land selection*

250 Agricultural class use was derived by thresholding the vegetation fraction by the same amount
251 in every image after performing SMA. Each vegetation fraction was classified by the binary
252 decision rule. The pixels that were more than the fixed threshold will be classified as
253 agricultural land; otherwise, they will be classified as non-agricultural (water, sand, rocks and
254 clay). The threshold was defined on the basis of the collected fractional vegetation coverage in
255 the field, visual interpretation and the exploitation of the high-resolution Google Earth images
256 to affine the binary classification.

257 *4.5. Accuracy assessment*

258 Evaluating vegetation fraction estimates can be challenging due to the difficulty of obtaining
259 reference data, especially for historical datasets. The land cover historical maps can be used to
260 assess the accuracy when the ground points of verification are absent. Unfortunately, after a
261 long research, we did not find the historical maps of Feija. Given the lack of high-quality
262 reference images from the 1980s, an accuracy assessment was only possible for 2017 using
263 Landsat OLI. We consider that the classification of the vegetation fraction from 1975 to 2016
264 would have acceptable accuracy if the vegetation fraction image in 2017 was reasonably
265 accurate.

266 For the accurate comparison of the differences between the estimated and the measured
267 fractional vegetation coverage, the coefficient of determination R^2 was used. Furthermore, the
268 accuracy of the binary classification was assessed using confusion matrix validation. A part of
269 the collected points was used in the initial phase of the SMA accuracy assessment, training and
270

272 binary classification of the vegetation (20 points). The other part was used for the confusion
273 matrix validation (18 points). The confusion matrix was estimated with reference to ground
274 reference data for producers, users and overall accuracy.

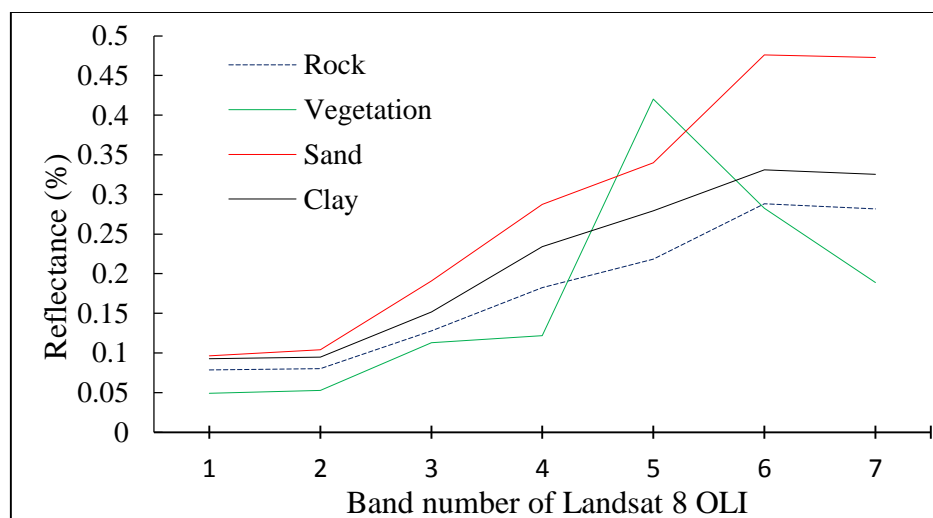
275 4.6. Driving forces of changes

276 This part discusses the extent to which the main factors contribute to the agricultural lands'
277 evolution. We conducted interviews with the local residents and stakeholders. The interviews
278 were consistent with the triggering events in the water harvesting management, economic
279 demand, agricultural policy changes and incentives. Several visits were made to the local
280 administrators. The interviews focused on agriculture policy change. For this purpose, 16
281 nomadic and 16 mainly sedentary households installed on communal pastoral land in the Feija
282 area were selected and visited in 2017.

283 5. Results

284 5.1. Results of endmembers and SMA

285 The application of PPI for each Landsat image allowed us to select four endmembers, which
286 are vegetation, clay, rock and sand. Given the analysis of the four spectral indices of the pure
287 pixels, rock, clay and sand had a similar spectral signature. Furthermore, the vegetation spectral
288 response was characterised by a pick between red and NIR bands (**Fig. 4**). This result implies
289 that the extraction of vegetated coverage can be easily distinguished from other features in the
290 Feija Area. The result of the SMA was an image with four abundances and a band of RMS
291 error. For each period, the RMS error was low (less than 0.02), indicating the pixel unmixing
292 results performed with high accuracies.



293
294 **Fig. 4.** Endmembers spectra of the Landsat OLI image.

295 After performing the SMA, we extracted the estimated coverage corresponding to each spatial
 296 position of field survey samples. Linear regression analysis was conducted between the
 297 measured and the estimated fractional vegetation for 20 points. The scatter plot of the accuracy
 298 assessment result presents a significant correlation ($R^2=0.90$) (**Fig. 5**).

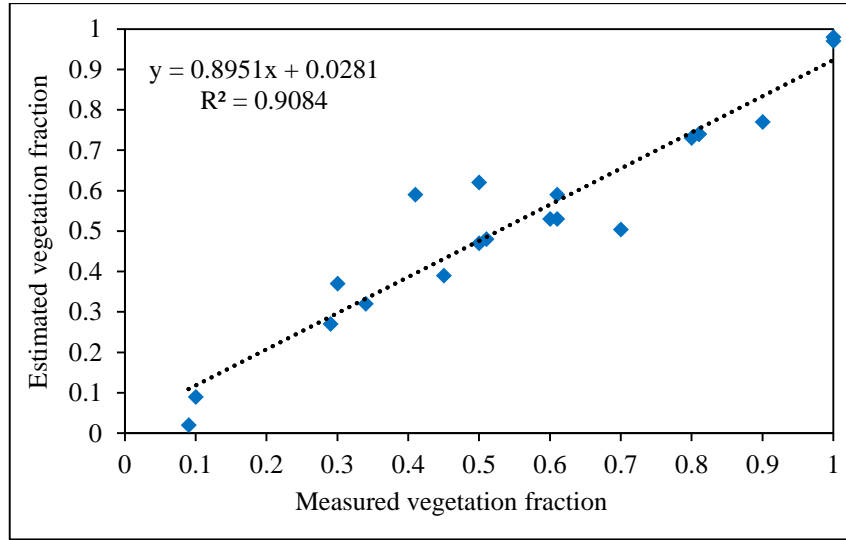


Fig. 5. Relationship between field survey data and estimated fractional vegetation.

5.2. Spatiotemporal evolution of agricultural land in the Feija Basin

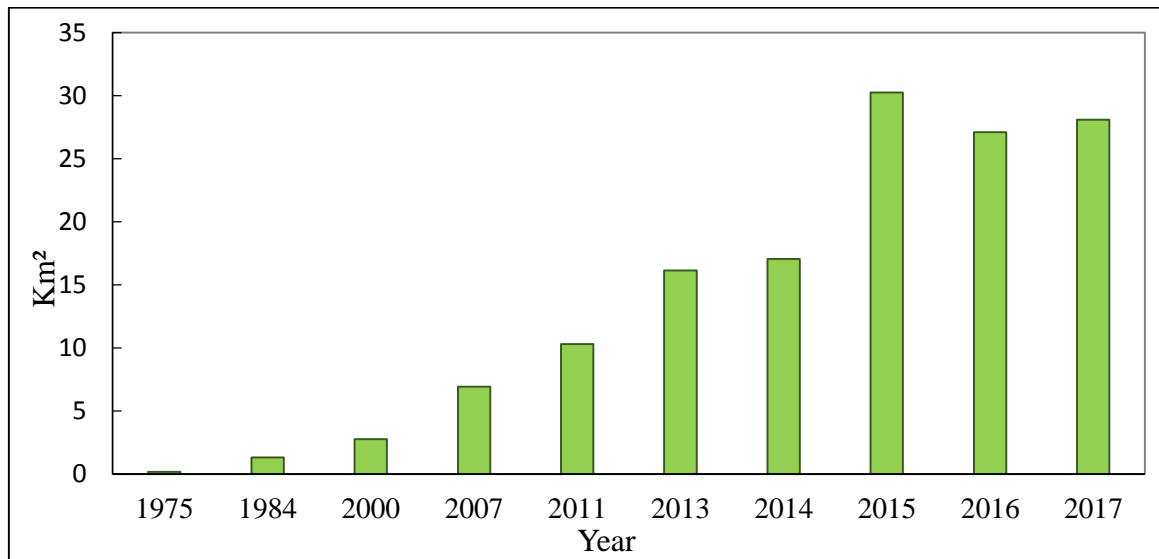
On the basis of the collected field vegetation coverage and Google Earth images, a threshold was terminated to separate the agricultural class with the other surface features, i.e. rangeland vegetation and barren lands. The class of agricultural land includes alfalfa, wheat, watermelon and date palm. A total of 30% of the vegetation was affirmed to have an accurate threshold that separates agricultural from the other land cover types. The classification accuracies are remarkably high due to the binary rule of a clear distinguishable feature.

The overall accuracy was calculated for the map of agricultural land of the Feija Area in 2017. The error matrix shows an overall accuracy of 94.4% (**Table 2**). No misclassification of nonagricultural samples into the agricultural class on the resulting map emerges. This illustrates that no commission error emerges in the agricultural class. However, an omission error in agricultural bounds emerges (only one pixel has been mapped as non-agricultural).

Table 2. Overall accuracy matrix for the agricultural land use map of the Feija Area in 2017.

		Reference data			User accuracy
		Agriculture	Non-agriculture	Total	
Map data	Agriculture	10	00	10	100.0 %
	Non-agriculture	01	07	08	87.5 %
	Total	11	07	18	–
Producer accuracy		90.9%	100.0%	–	94.4%

314 The evolution of agricultural area on the pastoral lands of Feija from 1975 to 2017, as a result
 1 315 of the binary classification tree, was presented in **Fig. 6**. The results demonstrate a rapid
 2 316 expansion over the time of the study. The total agricultural areas were 0.17 km² and 1.32 km²
 3 317 for 1975 and 1984, respectively, compared with 28.10 km² in June 2017. Ground observations
 4 318 revealed that these areas represent new farms within the former rangelands. The highest value
 5 319 of the agricultural land use surface was recorded in 2015 (30.25 km²).



320 **Fig. 6.** Evolution of the agricultural land use area (Km²) from 1975 to 2017.

321
 322 The agricultural class is displayed in the time steps 1984, 2007 and 2017. Figure.7 displays the
 323 spatial distribution of the agricultural land for 1984, 2007 and 2017. Spots with abundant
 324 vegetation occurred since 1984. These areas were totally non-existent in 1975. These spots
 325 appeared and increased remarkably in 2011. Ground observations revealed that these areas
 326 represent newly founded farms within the former rangelands.

327 The maps showed a rapid increase of farms in the north-east part of the study area, in Mgheder.
 328 Generally, the nearness to Zagora City was one of the reasons for the increasing farms in this
 329 region. New farmers prefer the areas near roads and cities for ease in selling products.

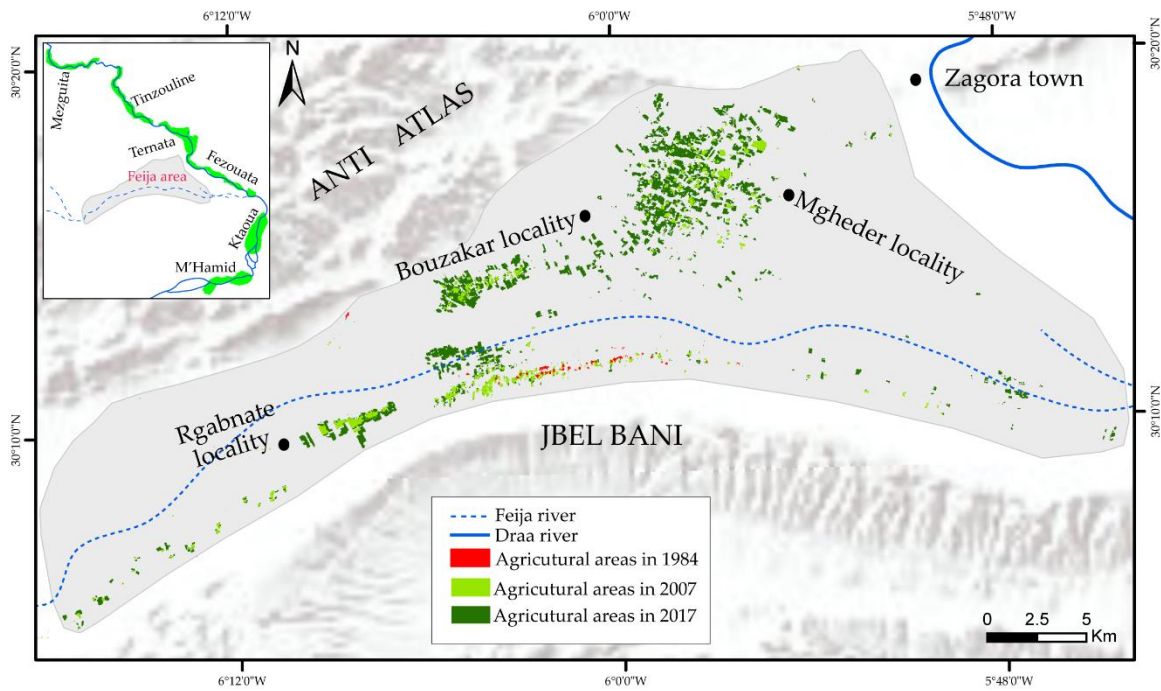


Fig. 7. Spatial distribution of the agricultural land use evolution in the Feija Area for 1984, 2007, and 2017.

6. Discussion

6.1. SMA and agricultural land use extraction in an arid context

The conditions in this arid pastoral area are suitable for the application of the SMA model due to the clear separability of the agriculture class from the other surface features and pastoral vegetation as expressed in the example of the four endmembers. This approach fits well when used to discriminate only green biomass, but it cannot be expected to fit other purposes, such as distinguishing among different soil types. However, SMA was proven to yield good performance, which is consistent with the other studies that have compared SMA with other fractional vegetation cover extraction models (Jia et al., 2017). It also provides a remarkable result for the mapping of agricultural lands (Peddle and Smith, 2005).

Previous studies analysed the oasis vegetation changes using spectral indices (NDVI) and Landsat images belonging from the previous sensors (Ait Lamqadem et al., 2017). In fact, applying the same threshold to separate vegetation and non-vegetation for the images from the different sensors is impossible. Given that during the last four decades the Landsat program employed different sensors and spectral band characteristics, SMA has proved to overcome the limitations of spectral indices.

351 *6.2. Spatial and temporal evolution of the agricultural land use*

1
2 352 The expansion was the main change trend exhibited by the agriculture class in the Feija Area
3
4 353 over the last 42 years. This situation is similar to the other arid pastoral areas across the world,
5
6 354 such as the cases of Kyrgyzstan and Kazakhstan (Rahimon, 2012), in the communal rangeland
7
8 355 grabbing in Sudan (Sulieman, 2018) and in China (Li et al., 2018). Generally, two stages can
9
10 356 be distinguished in this study. Firstly, the stage of 1975–2007 was characterized by a moderate
11
12 357 expansion in Feija. Secondly, the stage of 2007–2017 was characterized by a rapid expansion,
13
14 358 especially in the areas near the main road and Zagora City.

15 359 *6.3. Driving forces of changes*

16
17 360 The extracted extent of the irrigation lands shows a rapid expansion during the last two
18
19 361 decades. The number of inhabitants in the Feija Basin has increased rapidly during this period.
20
21 362 The number of population jumped from 20 inhabitants to 1572 from 1972 to 2014,
22
23 363 respectively (HCP, 2018). The sedentarisation of the pastoralists in this area can be
24
25 364 explained by the existence of water in the Feija River, pastoral land and a groundwater
26
27 365 characterized by its quality comparable with that of the oases in MDV. Furthermore, 78 new
28
29 366 farms were managed and created in the collective lands of the Feija Basin
30
31 367 between 1971 and 1985, and 169 news units were created from 1986 to 1997 (Proludra, 1998).
32
33 368 However, an updated census does not exist.

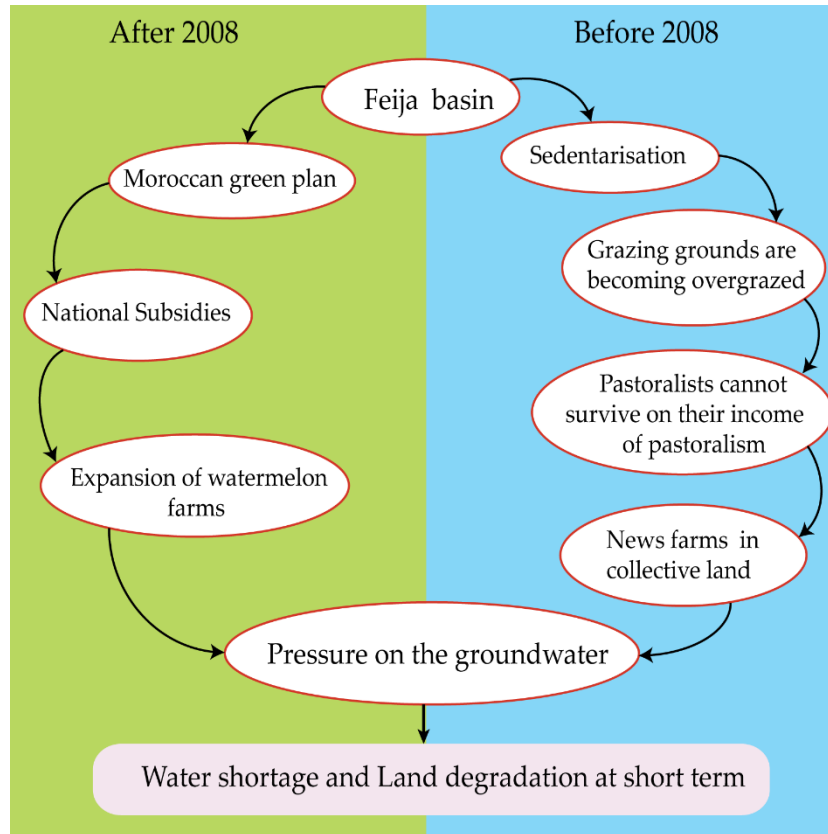
34
35 369 Several reasons can explain the sedentarisation in the study area. The pastoralists were coming
36
37 370 from the nearby regions of Feija within the 1000 km buffer zones, after each rainy period, by
38
39 371 vehicles. The results of the interviews prior to 2003 informed that the overgrazing in this area
40
41 372 increased the land degradation in the Feija Plain. Consequently, mobile pastoral can no longer
42
43 373 sustain grazing. Taking this into consideration plus the high cost of transportation, the
44
45 374 transformation of these pastoral lands into an irrigation areas deemed the only solution.

46 375 Regarding the climatic conditions, several drought episodes occurred in 1979–1984, 1987 and
47
48 376 1993–1995. This climatic factor accelerated the sedentarisation of mobile pastoralists (Ait
49
50 377 Lamqadem et al., 2018).

51
52 378 Pastoralists started the cultivation of henna as a secondary source of income before 2008 using
53
54 379 groundwater. However, this new form of farming does not solve overgrazing. Grazing was
55
56 380 continued in the neighbouring settlements because of their reduced of mobility. Farmers
57
58 381 reported scarcity of irrigation water, which had some negative effects. For some years, several

382 farmers had to deepen their wells from 2 to 5 m/year. In years of drought, cultivation in some
1 383 cases was no longer possible and farms had to be abandoned.

4 384 Starting 2008, Morocco launched the Moroccan Green Plan that gives subsidies to farmers in
5
6 385 Morocco to support agricultural activities. Figure 8 illustrates the consequences of overgrazing
7
8 386 and irrigation.



387
388 **Fig. 8.** Vicious circle deriving from farming on collective pastoral land

389 6.4. State policies and agricultural land use expansion

390 The number of farmers growing watermelon rapidly increased especially after 2010 as shown
391 in Figure 8 because of the development of new materials for drilling wells, motor-pumps and
392 the subsidies given to farmers under the Green Morocco Plan, which began in 2008. It was
393 introduced by the Ministry of Agriculture and Fisheries (Sedra, 2015; Sraïri, 2017). The Plan's
394 two pillars are for intensive farms and small subsistence farms or solidary agriculture.
395 According to the ORMVAO, the farmers in Feija benefited from the installation of dripping
396 irrigation and drilling wells. The Moroccan Green Plan gives subsidies to farmers to equip the
397 farms. Those subsidies can go up to 90%.

398 Since 2008, the cultivation of watermelon has spread in the southeast of Morocco to the
399 provinces of Ouarzazate and Zagora (where the Feija is located). Indeed, the favourable climatic

400 conditions increased the quality and yield of crops, guaranteeing a high selling price (MAPM,
401 2013). The results of the expansion of irrigation areas correlate with the official statistics of
402 Morocco. According to the Ministry of Agriculture and Fisheries, the cultivated area of
403 watermelon was increased from less than 100 ha in 2008 in the Zagora Province to 1100 ha in
404 2013 (MAPM, 2013).

405 Furthermore, the climatic and edaphic characteristics in the Feija Area favoured the cultivation
406 of watermelon. In fact, watermelon (*Citrullus vulgaris*) is endemic in arid zones. Watermelons
407 prefer an arid to a semiarid climate with average daily temperatures of 22 to 30 °C. The
408 maximum and minimum temperatures required for their development are approximately 20 to
409 35 °C (FAO, 1980), with sandy loam soil, which was found in the study area. Watermelons in
410 arid regions have a high content of sugar (FAO, 1980).

411 *6.5. Towards a good environmental management in Feija and in the MDV*

412 The watermelon farms can mobilise the local economy of the region because of the crops' added
413 value, which has created job opportunities for the younger generations. The use of groundwater
414 has two benefits for the locals, irrigation and drinking water supply for Zagora. The quality of
415 this water is good (low concentration of salinity) compared with the water in the groundwater
416 of the Ternata Oasis. In addition, the water in the Feija Basin is fresher than those of the other
417 oases and compared with the other groundwater at the MDV. On the basis of the analysis of the
418 collected water samples, the average water salinity in Feija was 1.09 g/l, against 2.51 g/l and
419 5.56 g/l for the Ternata and M'Hamid oases, respectively. The expansion of the irrigated areas
420 exerted pressure in the groundwater, thereby causing water scarcity in the area. The increasing
421 number of wells and motor pumps resulted in a negative groundwater balance estimated at –
422 1.3Mm³/a in 2006 (Klose and Reichert, 2006) and more than 5 Mm³/a in 2014 (ABHSM, 2014).
423 Between 1980 and 2014, the piezometric level showed a drawdown from 1 to 21 m, the high
424 values registered in the localities of Lamghadre and Bouzkar (ABHSM, 2014). During the field
425 visits and our interviews with locals, they affirmed that watermelons do not have any effect on
426 the environment. However, date palm trees planted in the areas of the quaternary water table
427 (rechargeable) must be taken into consideration, against the Feija Plain that is located in an area
428 with a deep water table (ABHSM, 1997).

429 In sum, damaging human practices were affirmed to be the dominant factor driving water
430 scarcity in the Feija Area in the past decades, characterized by the integration of new
431 cultivations that require large quantities of water, which leads to water scarcity. Water scarcity

432 in Zagora City was manifested by the shortage of drinking water in October 2017. This finding
1 433 is similar in to those in other countries, e.g. north of China (Wang et al., 2016), Jordan (Abu-
2 434 Allaban et al., 2015), West Africa (Klose and Reichert, 2006) and Egypt (Ouda, 2016; Zohry
3 435 and Ouda, 2016) with arid and Saharan climate, where water scarcity occurred due to the
4 436 expansion of irrigated areas and the overuse of groundwater.
5
6
7
8

9 437 In recent years, the cultural areas in the Feija basin has rapidly expanded, and the influence of
10 438 the damaging agricultural practices have accelerated, which will cause serious environmental
11 439 problems, such as groundwater recession, drinking water scarcity, land degradation by using
12 440 chemicals fertilizers (Badraoui, 2006) and wind erosion after each cropping season.
13 441 Furthermore, Morocco is severely affected by climate change (Brahim et al., 2017; Pascual et
14 442 al., 2017) with the consequences evident in the rising temperatures and decreasing
15 443 precipitations. The situation is getting aggravated in these arid areas. The government should
16 444 pay considerable attention to the fragile ecosystem, and we propose in this research to stop
17 445 cultivating watermelons in the Feija Basin and to adopt other cultivation with less water
18 446 consumption and with high added value in the market, e.g. medicinal and aromatic plants,
19 447 regeneration of old date palm in the oases and conversion of watermelon farmers to modern
20 448 palm date palm farms equipped with the drip irrigation system and a sustainable rangeland
21 449 governance for the remaining pastoral lands. To support this proposal, we compared the water
22 450 requirement to irrigate watermelon and palm tree cultivations. The irrigation of 1 ha of
23 451 watermelons requires 50,000 m³ of water, which is equivalent to 5 ha of date palm trees
24 452 (ABHSM, 2014). This estimate covers the period of 2017–2022. We then estimated the required
25 453 water for irrigation in two scenarios. The first scenario is if we continue cultivating watermelons
26 454 and the second is if we adopt the cultivation of palm trees. For the first scenario, the expected
27 455 agricultural land areas will reach 4758.77 ha in 2022, which needs 237.93M m³ to irrigate. If
28 456 we adopt palm trees instead of watermelon crops for the same area, then the needed amount of
29 457 water for irrigation is only 47.58M m³ (**Fig. 9**).
30
31
32
33
34
35
36
37
38
39
40
41
42
43
44
45
46
47
48
49
50
51
52
53
54
55
56
57
58
59
60
61
62
63
64
65

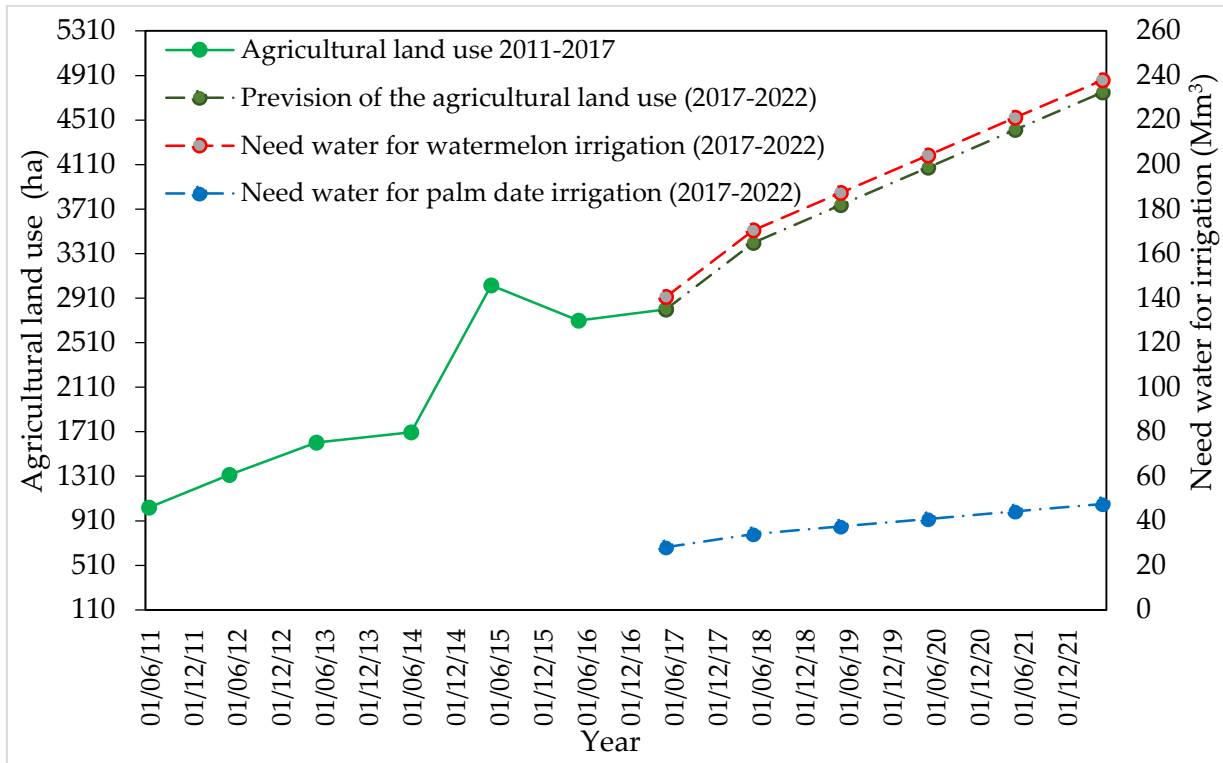


Fig. 9. Prevision of the agricultural land use for the period 2017–2022 and estimation of the needed water for irrigation for the cultivation of watermelon and palm date scenarios.

Furthermore, increasing the awareness of the local population to adopt good practices through research like ours can provide a solution for reducing the negative effect damaging agricultural practices in these fragile lands.

7. Conclusion

Historical remote sensing data from multi-sensors and geospatial tools were used to reconstruct the past and present conditions in the Feija Area and the driving forces of the changes and their effects to the environment over the last three decades. The use of SMA was useful to detect the changes between 1975 and 2017 in the land use in Feija. This long-term monitoring shows not only the pattern of changes but also the extent and degree of the impact of damaging practices on the environment, specifically in an arid area. This study reveals that rapid expansion was the dominant change in the last 33 years. This area has seen a transition from mobile pastoral to agricultural land use. The results corroborated that, in the long term, the inhabitants suffer from uncontrolled changes in the land use. People are forced to change their way of living to survive. The vegetation area increased rapidly during the last three decades in Feija from 1.23 km² in 1984 to 30.03 km² in June 2017. The expansion caused several environmental problems, such as water scarcity of the population of Zagora City and groundwater drawdown due to the intensity of irrigation. The socioeconomic situations of population, policy and economic interests were the driving forces of these changes in this area. The Feija Area and the arid areas

479 of Morocco need considerable attention and studies to protect and adopt good practices, which
480 are suitable for arid climatic conditions while considering the effects of climate change. The
481 limitations of the study lies in the lack of the historical image of land use/ land cover, and
482 accurate socio-economic data (precipitation, temperature, inhabitations number). In addition,
483 to improve the results of the fraction vegetation extraction in the arid areas, the new remote
484 sensing data of Sentienel-2 satellite could be a good alternative.

485 **Funding**

486 This research is supported by the Centre for Advanced Modelling and Geospatial Information
487 Systems (CAMGIS), University of Technology Sydney (UTS) under grant number
488 321740.2232335 and 321740.2232357.

489 **Acknowledgments**

490 We would like to thank the National Center of the Scientific and Technique Research for the
491 scholarship of PhD student A.A.L. (Scholarship N° 1UCD2016). Our acknowledgments are
492 also addressed to the Regional Office of the Agricultural Development for providing the
493 statistical data and WorldClim for the climate data. We thank the Chouaïb Doukkali University
494 for the logistical support during the field works of this study.

496 **References**

- 497 ABHSM (2014) Etude hydrologique de la nappe de la Feija. Agence des bassines hydrauliques de Souss
498 Mass, Direction de Ouarzazate, Ouarzazate, 38p.
- 499 ABHSM (1997) Etude d'approvisionnement en eau potable des populations rurales de la province de
500 Zagora. Agence des bassines hydrauliques de Souss Mass, Direction de Ouarzazate, Ouarzazate,
501 70 p.
- 502 Abu-Allaban M, El-Naqa A, Jaber M, Hammouri N (2015) Water scarcity impact of climate change in
503 semi-arid regions: a case study in Mujib basin, Jordan. Arab. J. Geosci. Vol. 8, 951-959 p.
504 <https://doi.org/10.1007/s12517-014-1266-5>.
- 505 Adams JB, Sabol D E, Kapos V, Almeida Filho R, Roberts D A, Smith M O, Gillespie A R (1995)
506 Classification of multispectral images based on fractions of endmembers: Application to land-
507 cover change in the Brazilian Amazon. Remote Sens. Environ. Vol. 52, 137-154 p.
508 [https://doi.org/10.1016/0034-4257\(94\)00098-8](https://doi.org/10.1016/0034-4257(94)00098-8)
- 509 Adams J B, Smith MO, Johnson P E (1986) Spectral mixture modeling: A new analysis of rock and soil
510 types at the Viking Lander 1 Site. J. Geophys. Res. Vol. 91, 8098- 8112 p.
511 <https://doi.org/10.1029/JB091iB08p08098>.
- 512 Afrasinei G M, Melis M T, Arras C, Pistis M, Buttau C, Ghiglieri G (2018) Spatiotemporal and spectral
513 analysis of sand encroachment dynamics in southern Tunisia. Eur. J. Remote Sens. Vol. 51, 352-
514 374 p. <https://doi.org/10.1080/22797254.2018.1439343>.

- 515 Ait Lamqadem A, Pradhan B, Saber H, Rahimi A (2018) Desertification Sensitivity Analysis Using
 1 516 MEDALUS Model and GIS: A Case Study of the Oases of Middle Draa Valley, Morocco. *Sensors*
 2 517 18: 2230. <https://doi.org/10.3390/S18072230>.
 3
- 4 518 Ait Lamqadem A, Saber H, Rahimi A (2017) Spatiotemporal Changes of Vegetation in the Middle Draa
 5 519 Valley Oasis : A Study Case of M ' hamid El Ghizlane Oasis (Morocco). *Eur. Sci. J.* 13: 115-132.
 6 520 <https://doi.org/10.19044/esj.2017.v13n24p115>.
 7
- 8 521 Allbed A, Kumar L, Sinha P (2014) Mapping and modelling spatial variation in soil salinity in the Al
 9 522 Hassa Oasis based on remote sensing indicators and regression techniques. *Remote Sens.* 6: 1137-
 10 523 1157. <https://doi.org/10.3390/rs6021137>.
 11
- 12 524 Badraoui M (2006) Connaissance et utilisation des ressources en sol au Maroc. Contribution in «
 13 525 Rapport sur le Développement Humain (RDH50) Maroc (50 ans de Développement Humain et
 14 526 perspectives 2025, Rapport Général)», report number: GT8-3. Publisher: Royal Institute for
 15 527 Strategic Studies (IRES). 91-117. <http://www.ires.ma/en/gt8-3-2/>
 16
- 17 528 Brahim YA, Saidi M E M, Kouraiss K, Sifeddine A, Bouchaou L (2017) Analysis of observed climate
 18 529 trends and high resolution scenarios for the 21st century in Morocco. 8: 1375-1384.
 19
- 20 530 Dawelbait M, Dal Ferro N, Morari F (2017) Using Landsat Images and Spectral Mixture Analysis to
 21 531 Assess Drivers of 21-Year LULC Changes in Sudan. *L. Degrad. Dev.* 28:116-127.
 22 532 <https://doi.org/10.1002/ldr.2556>.
 23
- 24 533 Elmore A J, Mustard J F, Manning S J, Lobell D B (2000) Quantifying Vegetation Change in Semiarid
 25 534 Environments: Precision and Accuracy of Spectral Mixture Analysis and the Normalized
 26 535 Difference Vegetation Index. *Remote Sens. Environ.* 73: 87102. [https://doi.org/10.1016/S0034-4257\(00\)00100-0](https://doi.org/10.1016/S0034-4257(00)00100-0).
 27 536
 28
- 29 537 FAO (2017) The future of food and agriculture - Trends and challenges. Rome, 180,
 30 538 <http://www.fao.org/3/a-i6583e.pdf>
 31
- 32 539 FAO (1980) Réponse des rendements à l'eau. F.A.O, 235.
 33
- 34 540 Faysse N (2015) The rationale of the Green Morocco Plan: missing links between goals and
 35 541 implementation. *J. North African Stud.* 20: 622-634.
 36 542 <https://doi.org/10.1080/13629387.2015.1053112>.
 37
- 38 543 Fernández-Manso Ó (2015) Spectral Mixture Analysis and Object- based Image Analysis for Forestry
 39 544 Applications. Doctoral Thesis, University of León.
 40
- 41 545 Foley J A, Ramankutty N, Brauman K A, Cassidy E S, Gerber J S, Johnston M, Mueller N D, O'Connell
 42 546 C, Ray D K, West P C, Balzer C, Bennett E M, Carpenter S R, Hill J, Monfreda C, Polasky S,
 43 547 Rockström J, Sheehan J, Siebert S, Tilman D, Zaks D P M (2011) Solutions for a cultivated planet.
 44 548 *Nature* 478: 337-342. <https://doi.org/10.1038/nature10452>.
 45
- 46 549 Guo Q, Fu B, Shi P, Cudahy T, Zhang J, Xu H (2017) Satellite Monitoring the Spatial-Temporal
 47 550 Dynamics of Desertification in Response to Climate Change and Human Activities across the
 48 551 Ordos Plateau, China. *Remote Sens.* 9: 525. <https://doi.org/10.3390/rs9060525>.
 49
- 50 552 Hamad R, Balzter H, Kolo K, Hamad R, Balzter H, Kolo K (2018) Predicting Land Use/Land Cover
 51 553 Changes Using a CA-Markov Model under Two Different Scenarios. *Sustainability* 10: 3421.
 52 554 <https://doi.org/10.3390/su10103421>.
 53
- 54 555 Han X, Han L (2015) Estimating Fractional Vegetation Cover of Oasis in Tarim Basin , China , Using
 55 556 Dimidiate Fractional Cover Model 9808, 1-8. <https://doi.org/10.1117/12.2204868>.
 56
- 57 557 HCP(2018) High Commission of the Plan of the Kingdom of Morocco. URL <https://www.hcp.ma/>
 58 558 (accessed 4.10.18).
 59
- 60 559 Jia K, Li Y, Liang S, Wei X, Yao Y (2017) Combining estimation of green vegetation fraction in an arid
 61
 62
 63
 64
 65

- 560 region from Landsat 7 ETM+ data. *Remote Sens.* 9: 1-15. <https://doi.org/10.3390/rs9111121>.
- 1
2 561 Kartya Y, Iwata S, Iinamura T (2005) Geomorphology and Pastoral-agricultural Land Use in Cotahuasi
3 562 and Puica, Southern Peruvian Andes. *Geogr. Rev. Jpn.* 78: 842-852.
4 563 <https://doi.org/10.4157/grj.78.842>.
- 5
6 564 Klose A (2009) Soil characteristics and soil erosion by water in a semi-arid catchment (Wadi Drâa,
7 565 South Morocco) under the pressure of global change. *Université de Bonn.* pp. 378.
- 8
9 566 Klose S, Reichert B (2006) Groundwater management in the middle Drâa-River basin (South-Morocco),
10 567 in: 14th International Soil Conservation Organization Conference. Marrakech, Morocco, pp. 1–4.
- 11 568 Li S, Sun Z, Tan M, Guo L, Zhang X (2018) Changing patterns in farming–pastoral ecotones in China
12 569 between 1990 and 2010. *Ecol. Indic.* 89: 110-117.
14 570 <https://doi.org/10.1016/J.ECOLIND.2018.01.067>.
- 15
16 571 Li Y, Wang H, Li X B (2015) Fractional Vegetation Cover Estimation Based on an Improved Selective
17 572 Endmember Spectral Mixture Model. *PLOS ONE* 10(4): e0124608.
18 573 <https://doi.org/10.1371/journal.pone.0124608>.
- 19
20 574 Long, J.A., Nelson, T.A., Wulder, M.A., 2010. Characterizing forest fragmentation: Distinguishing
21 575 change in composition from configuration. *Appl. Geogr.* 30: 426-435.
22 576 <https://doi.org/10.1016/J.APGEOG.2009.12.002>.
- 23
24 577 Lu D (2006) Spectral mixture analysis of ASTER images for examining the relationship between urban
25 578 thermal features and biophysical descriptors in Indianapolis, Indiana, USA. *Remote Sens. Environ.*
26 579 104: 157–167. <https://doi.org/10.1016/J.RSE.2005.11.015>.
- 27
28 580 Matinfar H R, Roodposhti M S (2012) Decision tree land use/land cover change detection of Khoram
29 581 Abad city using Landsat imagery and ancillary SRTM data. *Middle-East J. Sci. Res.* 13(8): 40454053
30
- 31 582 MAPM, 2013. Note de veille : Filière pastèque. Rabat, Morocco. pp. 19.
- 32
33 583 Masoud A A (2014) Predicting salt abundance in slightly saline soils from Landsat ETM + imagery
34 584 using Spectral Mixture Analysis and soil spectrometry. *Geoderma* 217-218: 45-56.
35 585 <https://doi.org/10.1016/J.GEODERMA.2013.10.027>.
- 36
37 586 McPeak J G, Little P D (2018) Mobile Peoples, Contested Borders: Land use Conflicts and Resolution
38 587 Mechanisms among Borana and Guji Communities, Southern Ethiopia. *World Dev.* 103: 119-132.
39 588 <https://doi.org/10.1016/j.worlddev.2017.10.001>
- 40
41 589 Medjani F, Aissani B, Labar S, Djidel M, Ducrot D, Masse A, Hamilton C M L (2017) Identifying saline
42 590 wetlands in an arid desert .climate using Landsat remote sensing imagery. *Application on Ouargla*
43 591 *Basin, southeastern Algeria. Arab. J. Geosci.* 10: 9-10. [https://doi.org/10.1007/s12517-017-2956-](https://doi.org/10.1007/s12517-017-2956-6)
44 592 [6.](https://doi.org/10.1007/s12517-017-2956-6)
- 45
46 593 Meusburger K, Bänninger D, Alewell C (2010) Estimating vegetation parameter for soil erosion
47 594 assessment in an alpine catchment by means of QuickBird imagery. *Int. J. Appl. Earth Obs. Geoinf.*
48 595 12: 201-207. <https://doi.org/10.1016/J.JAG.2010.02.009>.
- 49
50 596 Mihi A, Tarai N, Chenchouni H (2017) Can palm date plantations and oasisification be used as a proxy
51 597 to fi ght sustainably against desertification and sand encroachment in hot drylands ? *Ecol. Indic. in*
52 598 *press.* <https://doi.org/10.1016/j.ecolind.2017.11.027>.
- 53
54 599 Ouda S (2016) Major Crops and Water Scarcity in Egypt: Irrigation Water Management under Changing
55 600 Climate. *SpringerBriefs in Water Science and Technology.* Springer International Publishing,
56 601 Cham. pp. 126. <https://doi.org/10.1007/978-3-319-21771-0>.
- 57
58 602 Pascual D, Pla E, Fons J, Abdul-Malak D (2017) Climate Change Impacts on Water Availability and
59 603 Human Security in the Intercontinental Biosphere Reserve of the Mediterranean (Morocco-Spain),
60 604 in: *Environmental Change and Human Security in Africa and the Middle East.* Springer

605 International Publishing, Cham, pp. 75-93. https://doi.org/10.1007/978-3-319-45648-5_4.

- 1
2 606 Peddle D R, Smith A M (2005) Spectral mixture analysis of agricultural crops: Endmember validation
3 607 and biophysical estimation in potato plots. *Int. J. Remote Sens.* 26: 4959-4979.
4 608 <https://doi.org/10.1080/01431160500213979>.
- 5
6 609 Pons X, Pesquer L, Cristóbal J, González-Guerrero O (2014) Automatic and improved radiometric
7 610 correction of Landsat imagery using reference values from MODIS surface reflectance images. *Int. J.*
8 611 *Appl. Earth Obs. Geoinf.* 33: 243–254
9
- 10 612 Proludra (1998) Feija d’Imssouffa: Elements de Comprehension. DEDRA/GTZ, Zagora.pp. 63.
- 11
12 613 Rahimon R M (2012) Evolution of Land Use in Pastoral Culture in Central Asia with Special Reference
13 614 to Kyrgyzstan and Kazakhstan, in: *Rangeland Stewardship in Central Asia*. Springer Netherlands,
14 615 Dordrecht, pp. 51–67. https://doi.org/10.1007/978-94-007-5367-9_3.
- 15
16 616 Roy D P, Wulder M A, Loveland T R, Allen R G, Anderson M C, Helder D, Irons J R, Johnson D M,
17 617 Kennedy R, Scambos T A, Schaaf C B, Schott J R, Sheng Y, Vermote E F, Belward A S,
18 618 Bindschadler R, Cohen W B, Gao F, Hipple J D, Hostert P, Huntington, J, Justice, C.O., Kilic, A,
19 619 Kovalskyy V, Lee Z P, Lyburner L, Masek J G, McCorkel J, Shuai Y, Trezza R, Vogelmann J,
20 620 Wynne R H, Zhu Z (2014) Landsat-8: Science and product vision for terrestrial global change
21 621 research. *Remote Sens. Environ.* 145: 154–172. <https://doi.org/10.1016/J.RSE.2014.02.001>.
- 22
23 622 Salih A A M, Ganawa E-T, Elmahl A A (2017) Spectral mixture analysis (SMA) and change vector
24 623 analysis (CVA) methods for monitoring and mapping land degradation/desertification in arid and
25 624 semiarid areas (Sudan), using Landsat imagery. *Egypt. J. Remote Sens. Sp. Sci.* 20: S21-S29.
26 625 <https://doi.org/10.1016/J.EJRS.2016.12.008>.
- 27
28 626 Scarth P F, Röder A, Schmidt M (2010) Tracking grazing pressure and climate interaction - the role of
29 627 Landsat fractional cover in time series analysis, in: Ben, S., G, B. (Eds.), *Proceedings of the 15th*
30 628 *Australasian Remote Sensing and Photogrammetry Conference*. Alice Springs, Australia, pp. 13.
31 629 <https://doi.org/doi:10.6084/m9.figshare.94250>.
- 32
33 630 Schmidt M, Thamm H P, Menz G (2003) Long term vegetation change detection in an and environment
34 631 using LANDSAT data, in: *Geoinformation for European-Wide Integration*. Millpress, Rotterdam,
35 632 pp. 496.
- 36
37 633 Sedra M H (2015) Date Palm Status and Perspective in Morocco, in: *Date Palm Genetic Resources and*
38 634 *Utilization*. Springer Netherlands, Dordrecht, pp. 257–323. [https://doi.org/10.1007/978-94-017-](https://doi.org/10.1007/978-94-017-9694-1_8)
39 635 [9694-1_8](https://doi.org/10.1007/978-94-017-9694-1_8).
- 40
41 636 Smith M O, Johnson P E, Adams J B (1985) Quantitative determination of mineral types and abundances
42 637 from reflectance spectra using principal components analysis. *J. Geophys. Res.* 90: C797.
43 638 <https://doi.org/10.1029/JB090iS02p0C797>.
- 44
45 639 Smith MO, Ustin S L, Adams J B, Gillespie A R (1990) Vegetation in deserts: I. A regional measure of
46 640 abundance from multispectral images. *Remote Sens. Environ.* 31: 1–26.
47 641 [https://doi.org/10.1016/0034-4257\(90\)90074-V](https://doi.org/10.1016/0034-4257(90)90074-V).
- 48
49 642 Srairi, M.T., 2017. New challenges for the moroccan agricultural sector to cope with local and global
50 643 changes. Nova Science Publishers, Inc., pp. 165–188.
- 51
52 644 Sulieman H M (2018) Exploring the spatio-temporal processes of communal rangeland grabbing in
53 645 Sudan. *Pastoralism* 8(1): 14. <https://doi.org/10.1186/s13570-018-0117-5>.
- 54
55 646 Tang Z, Ma J, Peng H, Wang S, Wei J (2017) Spatiotemporal changes of vegetation and their responses
56 647 to temperature and precipitation in upper Shiyang river basin, *Advances in Space Research.* 6° (5):
57 648 969-979 COSPAR. <https://doi.org/10.1016/j.asr.2017.05.033>.
- 58
59 649 Teixido A L, Quintanilla L G, Carreño F, Gutiérrez D (2010) Impacts of changes in land use and
60
61
62
63
64
65

- 650 fragmentation patterns on Atlantic coastal forests in northern Spain. *J. Environ. Manage.* 91: 879–
1 651 886.
- 2
3 652 Tilman D, Clark M (2015) Food, Agriculture & the Environment: Can We Feed the World &
4 653 Save the Earth?. *Daedalus* 144: 8–23. https://doi.org/10.1162/DAED_a_00350.
- 5
6 654 Wang J, Huang Q, Huang J, Rozelle S, Wang J, Huang Q, Huang J, Rozelle S (2016) Water Scarcity in
7 655 Northern China, in: *Managing Water on China's Farms*. Elsevier, pp. 3–19.
8 656 <https://doi.org/10.1016/B978-0-12-805164-1.00001-4>.
- 9
10 657 Wang K, Franklin S E, Guo X, Cattet M (2010) Remote Sensing of Ecology, Biodiversity and
11 658 Conservation: A Review from the Perspective of Remote Sensing Specialists. *Sensors* 10: 9647-
12 659 9667. <https://doi.org/10.3390/s101109647>.
- 13
14 660 White M A, Asner G P, Nemani R R, Privette, J L, Running S W (2000) Measuring Fractional Cover
15 661 and Leaf Area Index in Arid Ecosystems: Digital Camera, Radiation Transmittance, and Laser
16 662 Altimetry Methods. *Remote Sens. Environ.* 74:45-57. [https://doi.org/10.1016/S0034-4257\(00\)00119-X](https://doi.org/10.1016/S0034-4257(00)00119-X).
- 17 663
18
19 664 Xie H, He Y, Zhang N, Lu H (2017) Spatiotemporal changes and fragmentation of forest land in Jiangxi
20 665 Province, China. *Journal of Forest Economics*. Elsevier GmbH. 29 (1): 4-13
21 666 <https://doi.org/10.1016/j.jfe.2017.08.004>.
- 22
23 667 Xofis P, Poirazidis K (2018) Combining different spatio-temporal resolution images to depict landscape
24 668 dynamics and guide wildlife management. *Biol. Conserv.* 218:10-17.
25 669 <https://doi.org/10.1016/j.biocon.2017.12.003>.
- 26
27 670 Yıldırım A, Öner M D (2015) Electrical Conductivity, Water Absorption, Leaching, and Color Change
28 671 of Chickpea (*Cicer arietinum* L.) during Soaking with Ultrasound Treatment. *Int. J. Food Prop.*
29 672 18: 1359-1372. <https://doi.org/10.1080/10942912.2014.917660>.
- 30
31 673 Zainabi A T (1989) Vers une disparition rapide du nomadisme au Sahara marocain : Le cas du Dra
32 674 Moyen, in: Urmba (Ed.), *Le Nomade, l'oasis et La Ville*. Urbama, pp. 49–62.
- 33
34 675 Zhang, X., Liao, C., Li, J., Sun, Q., 2013. Fractional vegetation cover estimation in arid and semi-arid
35 676 environments using HJ-1 satellite hyperspectral data. *Int. J. Appl. Earth Obs. Geoinf.* 21: 506-512.
36 677 <https://doi.org/10.1016/J.JAG.2012.07.003>.
- 37
38 678 Zhang X, Luo Y, Goh K S (2018) Modeling spray drift and runoff-related inputs of pesticides to
39 679 receiving water. *Environ. Pollut.* 234: 48-58. <https://doi.org/10.1016/j.envpol.2017.11.032>.
- 40
41 680 Zhu Z (2017) Change detection using landsat time series: A review of frequencies, preprocessing,
42 681 algorithms, and applications. *ISPRS J. Photogramm. Remote Sens.* 130: 370-384.
43 682 <https://doi.org/10.1016/j.isprsjprs.2017.06.013>.
- 44
45 683 Zohry A E-H, Ouda S A H (2016) Crops Intensification to Face Climate Induced Water Scarcity in
46 684 Nile Delta Region. In: *Management of Climate Induced Drought and Water Scarcity in Egypt*.
47 685 SpringerBriefs in Environmental Science. Springer, Cham. pp. 47-62. https://doi.org/10.1007/978-3-319-33660-2_4.
- 48 686
49
50
51 687
52
53
54
55
56
57
58
59
60
61
62
63
64
65